Pramana – J. Phys. (2017) 89:27
DOI 10.1007/s12043-017-1419-7

Recent observational constraints on EoS parameters of a class of emergent Universe

P THAKUR

Physics Department, Alipurduar College, Alipurduar 736 122, India
E-mail: prasenjit_thakur1@yahoo.co.in

MS received 13 October 2016; revised 19 December 2016; accepted 25 January 2017;
published online 20 July 2017

Abstract. Emergent Universe (EU) model is investigated here using the recent observational data of the background tests. The background test data comprise observed Hubble data, baryon acoustic oscillation data, cosmic microwave background shift data and Union compilation(2.1) data. The flat EU model obtained by Mukherjee *et al* is permitted with a non-linear equation of state (in short, EoS) ($p = A\rho - B\rho^{1/2}$), where A and B are constants. The best-fit values and permitted range of values of the EoS parameters are determined in general EU model and in specific EU model ($A = 0$) by using chi-square minimization technique. The best-fit values of the EoS parameters are used to study the evolution of the squared adiabatic sound speed c_s^2, state parameter ω and deceleration parameter q for different red-shifts z. The present age of the Universe t_0 has been determined in general EU model as well as for EU model with $A = 0$. The late accelerating phase of the Universe in the EU model is accommodated satisfactorily.

Keywords. Cosmology; dark energy; dark matter; large-scale structures.

PACS Nos 98.80.−k; 95.36.+x; 95.35.+d; 98.65.Dx

1. Introduction

After the discovery of cosmic microwave background radiation [1,2], the Big-Bang model became the Standard Model of the Universe which has a beginning at some finite past. However, Big-Bang model based on perfect fluid assumptions fails to account for some of the observed facts of the Universe. Further, it is observed that while probing the early Universe, a number of problems namely, the horizon problem, flatness problem and singularity problem, cropped up. In order to resolve those issues of the early Universe, the concept of inflation [3–6] was introduced in cosmology. These inflationary models could not solve the initial singularity problem. Another mystery is the observational prediction of accelerating Universe [7–10]. This phase of acceleration which is a late-time phenomenon of the Universe, can be accommodated in the Standard Model with the introduction of a positive cosmological constant. However, the physics of the inflation and introduction of a small cosmological constant for late-time acceleration, is not clearly understood [11,12]. In the literature, the late accelerating phase of the Universe is obtained with exotic matter or with a modification of the Einstein gravity. A non-linear equation of state is also considered in the literature to construct cosmologies [13], and emergent Universe (EU) model is one such model. The EU model obtained by Mukherjee *et al* in the flat Universe permits an accelerating phase.

The EU starts from a static Einstein Universe thereby avoiding the messy situation of the initial singularity [14,15] and afterward successfully accommodates the accelerating phase. In the EU model, the late-time de-Sitter phase exists which naturally incorporates the late-time accelerating phase as well. EU scenario has been explored with quintom matter [16] and the realization of the scenario with a non-conventional fermion field was further investigated to obtain a scale-invariant perturbation [17]. It has been shown that the EU scenario can be implemented successfully in the framework of general relativity [13] in addition to Gauss–Bonnet gravity [18]. The modified Gauss–Bonnet gravity as gravitational alternative for dark energy is however considered by Nojiri and Oddintsov [19]. It is also shown recently that EU model can be successfully implemented in brane-world gravity [20,21], Brans–Dicke theory [22]. A number of cosmological models are obtained with different cosmological fluids and fields [14,23–25]

where initial singularity problem is addressed. Mukherjee *et al* [13] obtained an EU model in the framework of GTR with a polytropic equation of state (EoS) given by

$$p = A\rho - B\rho^{1/2}, \tag{1}$$

where A, B are constants with $B > 0$. This EU model is interesting as it avoids the initial singularity and accommodates the late-accelerating phase. The EoS parameters in the model play important roles which decide the composition of matter in the Universe. In ref. [13], it is shown that for a discrete set of values of A, namely, $A\left(=0, -\frac{1}{3}, \frac{1}{3}, 1\right)$, one obtains Universe with a mixture of three different kinds of cosmic fluids. Each of the above EU model has dark energy as one of its constituents. A study on EU model has been performed to determine the parameters from cosmological observations.

The analysis adopted here consists of four main background tests.

(1) The differential age of old galaxies, given by $H(z)$.
(2) The peak position of the baryonic acoustic oscillations (BAO).
(3) The CMB shift parameter.
(4) The SN Ia data. $H(z)-z$ data are given in table 1. The supernovae data are taken from the union compilation data (Union2.1) [26].

The paper is presented as follows: In §2, relevant field equations obtained from Einstein field equations are given. In §3, constraints on the EoS parameters obtained from background tests are presented. In §4, age in EU models are calculated. In §5, a summary of the results are noted. Finally, in §6, a brief discussion is given.

2. Field equations

The Einstein field equation is given by

$$R_{\mu\nu} - \frac{1}{2}g_{\mu\nu}R = 8\pi G T_{\mu\nu}, \tag{2}$$

where $R_{\mu\nu}$ represents Ricci tensor, R represents Ricci scalar, $T_{\mu\nu}$ represents energy–momentum tensor and $g_{\mu\nu}$ represents the metric tensor in four dimensions. Here, Robertson–Walker metric is considered which is given by

$$\mathrm{d}s^2 = -\mathrm{d}t^2 + a^2(t)\left[\frac{\mathrm{d}r^2}{1-kr^2} + r^2(\mathrm{d}\theta^2 + \sin^2\,\theta\,\mathrm{d}\phi^2)\right], \tag{3}$$

where $k = 0, +1(-1)$ is the curvature parameter in the spatial section representing flat, closed (open) Universe respectively and $a(t)$ is the scale factor of the Universe with r, θ, ϕ the dimensionless co-moving coordinates.

Using metric (3) in the Einstein field equation (2), the following equations are obtained:

$$3\left(\frac{\dot{a}^2}{a^2} + \frac{k}{a^2}\right) = 8\pi G\rho, \tag{4}$$

$$2\frac{\ddot{a}}{a} + \frac{\dot{a}^2}{a^2} + \frac{k}{a^2} = -8\pi G p, \tag{5}$$

where ρ and p represent the energy density and pressure respectively. The conservation equation is given by

$$\frac{\mathrm{d}\rho}{\mathrm{d}t} + 3H(\rho + p) = 0, \tag{6}$$

where $H = \dot{a}/a$ is the Hubble parameter. Using EoS given by eq. (1) in eq. (6), and integrating once, the expression for energy density is obtained as

$$\rho_{eu} = \left[\frac{B}{1+A} + \frac{1}{A+1}\frac{K}{a^{3(A+1)/2}}\right]^2, \tag{7}$$

where K is a positive integration constant. For convenience, eq. (7) is rewritten as

$$\rho_{eu} = \rho_{eu0}\left[A_s + \frac{1-A_s}{a^{3(A+1)/2}}\right]^2, \tag{8}$$

where

$$A_s = \frac{B}{1+A}\frac{1}{\rho_{eu0}^{1/2}}$$

and

$$\frac{K}{A+1} = \rho_{eu0}^{1/2} - \frac{B}{A+1}.$$

The scale factor of the Universe can be expressed as $a/a_0 = 1/(1+z)$, where z is the red-shift parameter and the present scale factor of the Universe is chosen to be $a_0 = 1$. Therefore, the Hubble parameter in terms of red-shift parameter can be rewritten using the field eq. (4) as

$$H(z) = H_0\left[A_s + (1-A_s)(1+z)^{3(A+1)/2}\right], \tag{9}$$

where H_0 represents the present Hubble parameter. Using the present matter density of the Universe $\Omega_m = (1-A_s)^2$ [27], Hubble parameter can be expressed as

$$H(z) = H_0\left[(1-\sqrt{\Omega_m}) + \sqrt{\Omega_m}(1+z)^{3(A+1)/2}\right]. \tag{10}$$

The square of the speed of sound is given by

$$c_s^2 = \frac{\delta p}{\delta\rho} = \frac{\dot{p}}{\dot{\rho}} \tag{11}$$

which reduces to

$$c_s^2 = A - \frac{(1-\sqrt{\Omega_m})(1+A)}{2(1-\sqrt{\Omega_m}+\sqrt{\Omega_m}(1+z)^{3(A+1)/2})}. \quad (12)$$

In terms of the state parameter, it reduces to

$$c_s^2 = \frac{\omega + A}{2}. \quad (13)$$

From the above equation, the inequality takes the form

$$\left(1-\sqrt{\Omega_m}\right) < 2\frac{A}{A+1} \quad (14)$$

for a realistic solution which admits stable perturbation [28]. Again, positivity of sound speed leads to an upper bound on $c_s^2 \leq 1$ which arises from the causality condition.

The deceleration parameter is given by

$$q(a) = \frac{\Omega_{eu}(a)[1+3\omega(a)]}{2[\Omega_{eu}(a)]}, \quad (15)$$

where

$$\Omega_{eu}(a) = \Omega_{eu0}\left[1-\sqrt{\Omega_m}+\frac{\sqrt{\Omega_m}}{a^{3(A+1)/2}}\right]^2. \quad (16)$$

3. Observational constraints

The EoS for the EU contains three unknown parameters, namely H_0, Ω_m and A, which are determined from numerical analysis. For this, the Einstein field equation is rewritten in terms of a dimensionless Hubble parameter and a suitable chi-square function is defined in different cases.

Case I: For OHD

The observed Hubble data (OHD) is then taken from the table given below: To analyse, first chi-square χ^2_{H-z} function is defined as

$$\chi^2_{\mathrm{OHD}}(H_0, \Omega_m, A) = \sum \frac{(H(H_0, \Omega_m, A, z) - H_{\mathrm{obs}}(z))^2}{\sigma_z^2}, \quad (17)$$

where $H_{\mathrm{obs}}(z)$ is the observed Hubble parameter at red-shift z and σ_z is the error associated with that particular observation as shown in table 1.

Case II: For BAO data

A model-independent BAO peak parameter for low red-shift z_1 measurements in a flat Universe is given by [29]

$$\mathcal{A}(\Omega_m, A, z_1) = \frac{\sqrt{\Omega_m}}{E(z_1)^{1/3}}\left(\frac{\int_0^{z_1} \mathrm{d}z/E(z)}{z_1}\right)^{2/3}, \quad (18)$$

where Ω_m is the present matter density parameter for the Universe. The chi-square function in this case is defined as

$$\chi^2_{\mathrm{BAO}}(\Omega_m, A) = \sum \frac{(\mathcal{A}(\Omega_m, A, z_1) - \mathcal{A}_{\mathrm{obs}}(z_1))^2}{(\sigma_{\mathcal{A}})^2}. \quad (19)$$

The BAO data are given in table 2.

Table 1. Observed Hubble data (OHD).

z	$H(z)$	σ	References	z	$H(z)$	σ	References
0.0708	79.0	±19.68	[31]	0.593	104.0	±13.0	[34]
0.09	69.0	±12.0	[32]	0.60	87.9	±6.1	[38]
0.12	68.6	±26.2	[31]	0.68	92.0	±8.0	[34]
0.17	83.0	±8.0	[33]	0.73	97.3	±7.0	[38]
0.179	75.0	±4.0	[34]	0.781	105.0	±12.0	[34]
0.199	75.0	±5.0	[34]	0.875	125.0	±17.0	[34]
0.20	72.9	±29.6	[31]	0.88	90.0	±40.0	[39]
0.240	79.69	±2.65	[35]	0.90	117.0	±23.0	[33]
0.27	77.0	±14.0	[33]	1.037	154.0	±20.0	[34]
0.28	88.8	±36.6	[31]	1.30	168.0	±17.0	[33]
0.35	82.1	+4.8, −4.9	[36]	1.363	160.0	±33.6	[41]
0.35	84.4	±7.0	[37]	1.43	177.0	±18.0	[33]
0.352	83.0	± 14.0	[34]	1.53	140.0	±14.0	[33]
0.40	95.0	±17.0	[33]	1.75	202.0	±40.0	[33]
0.43	86.45	±3.68	[35]	1.965	186.5	±50.4	[41]
0.44	82.6	±7.80	[38]	2.3	224.0	±8.0	[42]
0.48	97.0	±62.0	[39]	2.34	222.0	±7.0	[43]
0.57	92.4	±4.5	[40]	2.36	226.0	±8.0	[44]

Table 2. BAO data.

z_1	$\mathcal{A}$	$\sigma_{\mathcal{A}}$	References
0.106	0.526	0.028	[45]
0.20	0.488	0.016	[45]
0.35	0.484	0.016	[45]
0.44	0.474	0.034	[46]
0.57	0.436	0.017	[45,47]
0.60	0.442	0.020	[46]
0.73	0.424	0.021	[46]

Case III: For CMB

The CMB shift parameter ($\mathcal{R}$) is given by [30]

$$\mathcal{R} = \sqrt{\Omega_m} \int_0^{z_{\rm ls}} \frac{{\rm d}z'}{H(z')/H_0}, \tag{20}$$

where $z_{\rm ls}$ is the z at the surface of last scattering. The WMAP7 data predict $\mathcal{R} = 1.726 \pm 0.018$ at $z = 1091.3$. Now, chi-square function takes the form

$$\chi^2_{\rm CMB}(\Omega_m, A) = \frac{(\mathcal{R} - 1.726)^2}{(0.018)^2}. \tag{21}$$

Case IV: For supernovae data

The distance modulus function (μ) is defined in terms of luminosity distance ($d_{\rm L}$) as

$$\mu(H_0, \Omega_m, A, z) = m - M = 5\log_{10}(d_{\rm L}) + 25, \tag{22}$$

where

$$d_{\rm L} = \frac{c(1+z)}{H_0} \int_0^z \frac{{\rm d}z'}{E(z')}. \tag{23}$$

In this case, the chi-square χ^2_μ function is defined as

$$\chi^2_\mu(H_0, \Omega_m, A) = \sum \frac{(\mu(H_0, \Omega_m, A, z) - \mu_{\rm obs}(z))^2}{\sigma_z^2}, \tag{24}$$

where $\mu_{\rm obs}(z)$ is the observed distance modulus at redshift z and σ_z is the corresponding error for the 580 observed data [26]. Finally, the chi-square function for the background tests is defined as

$$\begin{aligned}\chi^2_{\rm back}(H_0, \Omega_m, A) &= \chi^2_{\rm OHD}(H_0, \Omega_m, A) + \chi^2_{\rm BAO}(\Omega_m, A) \\ &\quad + \chi^2_{\rm CMB}(\Omega_m, A) + \chi^2_\mu(H_0, \Omega_m, A).\end{aligned} \tag{25}$$

The chi-square function for the background test is utilized for the determination of EoS parameters, H_0, A and Ω_m.

3.1 *Observational constraints from background tests*

Likelihood function (L) is related to the chi-square for the background test as $L \propto \exp(-\chi^2_{\rm back}/2)$. To get the best-fit values of the EU model, likelihood function can be maximized or the chi-square function can be minimized. In this case, the best-fit values are obtained by minimizing the chi-square function. Since chi-square function depends on H_0, A and Ω_m, it is possible to draw contours at different confidence limits. The contours among the parameters H_0, A and Ω_m for background tests are shown in figure 1. The plot of the maximum likelihood functions with the parameters H_0, A and Ω_m for background test are shown in figure 2. The plot of

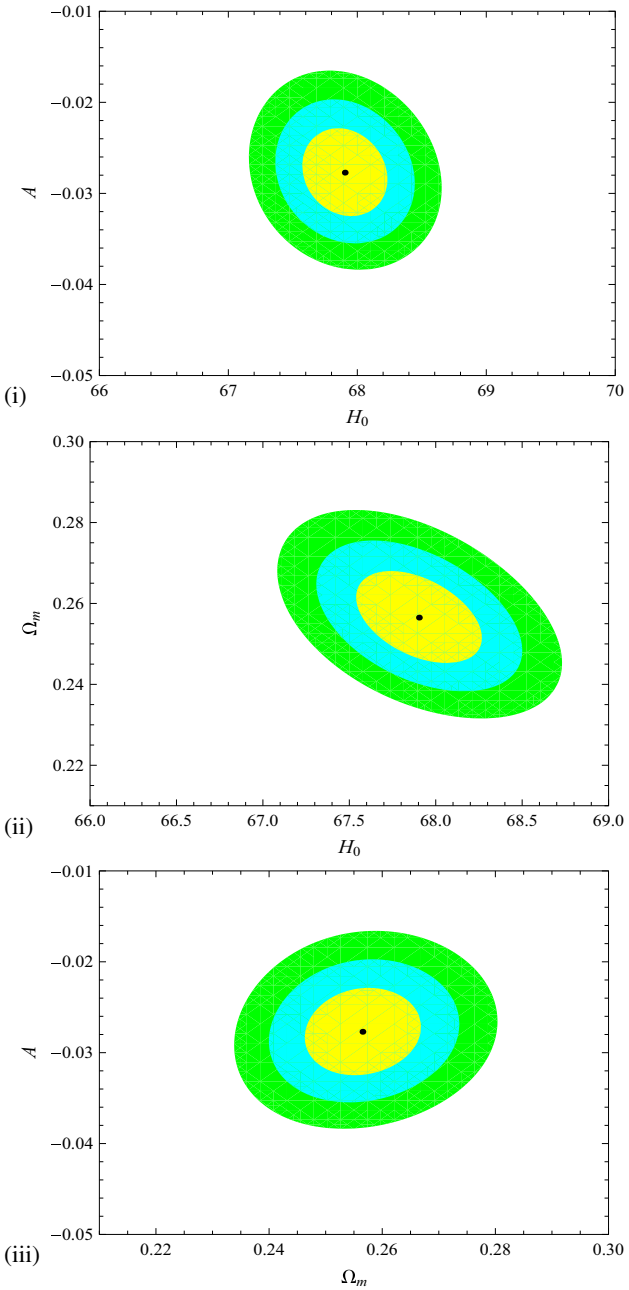

Figure 1. Contours of (**i**) H_0–A, (**ii**) H_0–Ω_m and (**iii**) Ω_m–A from OU data for the general EU model at 68.3% (yellow), 95.4% (blue) and 99.7% (green) confidence limits, where OU = OHD + BAO + CMB + Union2.1.

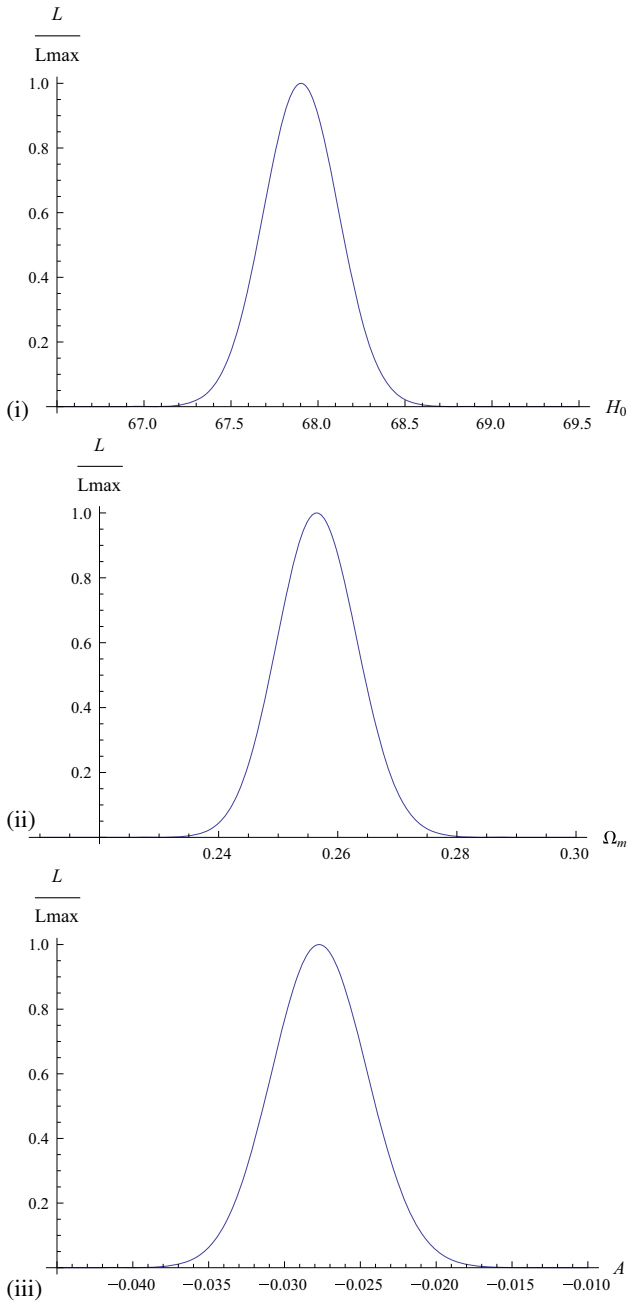

Figure 2. Plot of maximum likelihood functions with (**i**) H_0, (**ii**) Ω_m and (**iii**) A in the general EU model from OU data, where OU = OHD + BAO + CMB + Union2.1.

maximum likelihood functions with the parameters H_0 and Ω_m for the background test for $A = 0$ are shown in figure 3.

4. Age of the Universe in the EU model

The present age of the Universe is given as

$$t_0 = \int_0^1 \left[\frac{\mathrm{d}a}{aH(a)}\right], \tag{26}$$

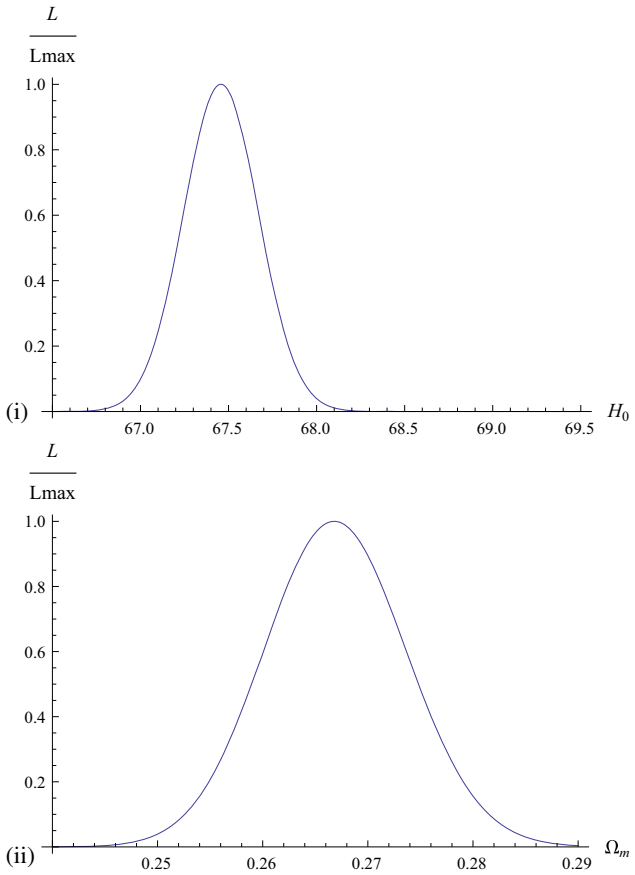

Figure 3. Plot of maximum likelihood functions with (**i**) H_0 and (**ii**) Ω_m in EU model with $A = 0$ from OU data.

where $(a/a_0) = 1/(1+z)$. In terms of $H(z)$ it is given in the EU model as

$$t_0 = \frac{1}{H_0}\int_0^{\inf}\left[\frac{\mathrm{d}z}{(1+z)f(\Omega_m, A, z)}\right] \tag{27}$$

with

$$f(\Omega_m, A, z) = \frac{H(z)}{H_0} \tag{28}$$

and $H(z)$ is given by eq. (10).

5. Results

In this analysis, the present Hubble parameter is also taken as a free parameter. So here H_0, A and Ω_m are the three parameters whose values are determined at different confidence levels. The best-fit values of the model obtained with background data are $H_0 = 67.90$, $A = -0.028$ and $\Omega_m = 0.256$ (shown in table 3). The permitted ranges at 68.3% confidence level (1σ) of the model obtained with background data are $H_0 = 67.90^{+0.33}_{-0.33}$, $A = -0.028^{-0.005}_{+0.005}$ and $\Omega_m = 0.256^{+0.012}_{-0.011}$

Table 3. Best-fit values of the EoS parameters from OU data in the EU model.

Data	H_0	A	Ω_m	χ^2/d.o.f.
OU	67.90	−0.028	0.256	1.182

Table 4. Range of values of H_0 and A from OU data in the EU model.

Data	CL (%)	H_0	A
OU	68.3	(67.57, 68.23)	(−0.033, −0.023)
OU	95.4	(67.36, 68.46)	(−0.036, −0.020)
OU	99.7	(67.16, 68.66)	(−0.038, −0.017)

Table 5. Range of values of H_0 and Ω_m from OU data in the general EU model.

Data	CL (%)	H_0	Ω_m
OU	68.3	(67.53, 68.26)	(0.245, 0.268)
OU	95.4	(67.30, 68.50)	(0.238, 0.276)
OU	99.7	(67.09, 68.72)	(0.231, 0.283)

Table 6. Range of values of Ω_m and A from OU data in the general EU model.

Data	CL (%)	Ω_m	A
OU	68.3	(0.246, 0.267)	(−0.033, −0.023)
OU	95.4	(0.240, 0.274)	(−0.036, −0.012)
OU	99.7	(0.234, 0.280)	(−0.038, −0.017)

Table 7. Best-fit values of EoS parameters in the general EU model in OU data.

Model	ω_0	q
EU	−0.515	−0.271

(tables 4–6). The acceptable ranges in the background test for the parameters H_0, A and Ω_m at 99.7% confidence level (3σ) are (67.09, 68.72), (−0.038, −0.017) and (0.231, 0.283) (which are shown in figure 1 and in tables 4–6). The present values of the parameters ω_0 and q in this EU model are −0.515 and −0.271 respectively (shown in table 7).

The best-fit values of the EU model with $A = 0$ obtained with background data are $H_0 = 67.457$ and $\Omega_m = 0.267$ (shown in table 8). The acceptable ranges in the background for the parameters H_0 and Ω_m at 99.7% confidence level (3σ) are (66.64, 68.29) and (0.242, 0.294) respectively (shown in figure 4 and table 9). The present values of the parameters ω_0 and q in this EU model are −0.485 and −0.226 respectively

Table 8. Best-fit values of the EoS parameters from OU data for $A = 0$ model.

Data	H_0	Ω_m	χ^2/d.o.f.
OU	67.457	0.267	1.287

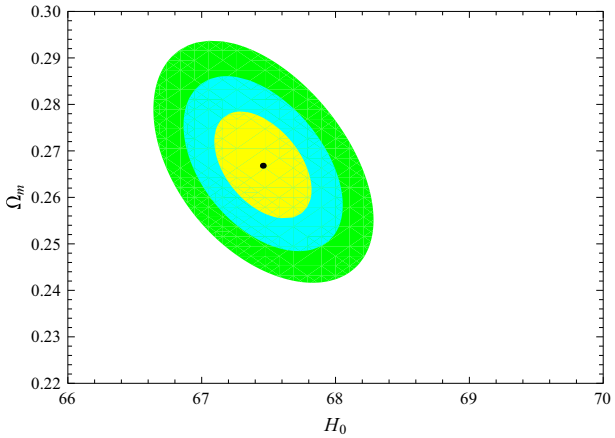

Figure 4. Contours of H_0–Ω_m in the EU model with $A = 0$ from OU data at 68.3% (yellow), 95.4% (blue) and 99.7% (green) confidence limit.

Table 9. Range of values of H_0 and Ω_m from OU data in the EU model with $A = 0$.

Data	CL (%)	H_0	Ω_m
OU	68.3	(67.09, 67.80)	(0.255, 0.279)
OU	95.4	(66.86, 68.06)	(0.248, 0.286)
OU	99.7	(66.64, 68.29)	(0.242, 0.294)

Table 10. Best-fit values of EoS parameters from OU data in the EU model with $A = 0$.

Model	ω_0	q
EU	−0.485	−0.226

(shown in table 10). The plot of likelihood functions in both the scenario are plotted in figures 2 and 3.

6. Discussion

In this paper, an analysis of the flat EU model [13] and the EU model with $A = 0$ with observational data has been performed. The following points are noted:

(i) The best-fit values and range of values obtained with the background data for the EU models considered are very close to each other. The best-fit values obtained with background data

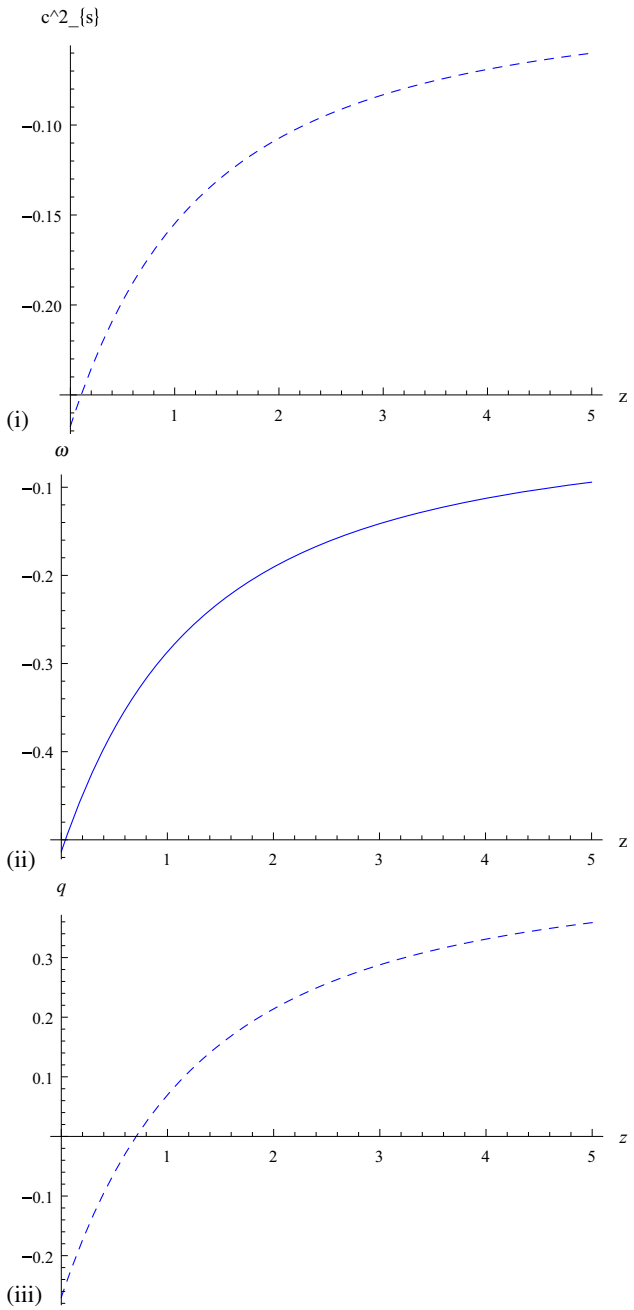

Figure 5. Evolution of (**i**) the squared adiabatic sound speed c_s^2, (**ii**) state parameter ω and (**iii**) deceleration parameter q with red shift in the general EU model from OU data.

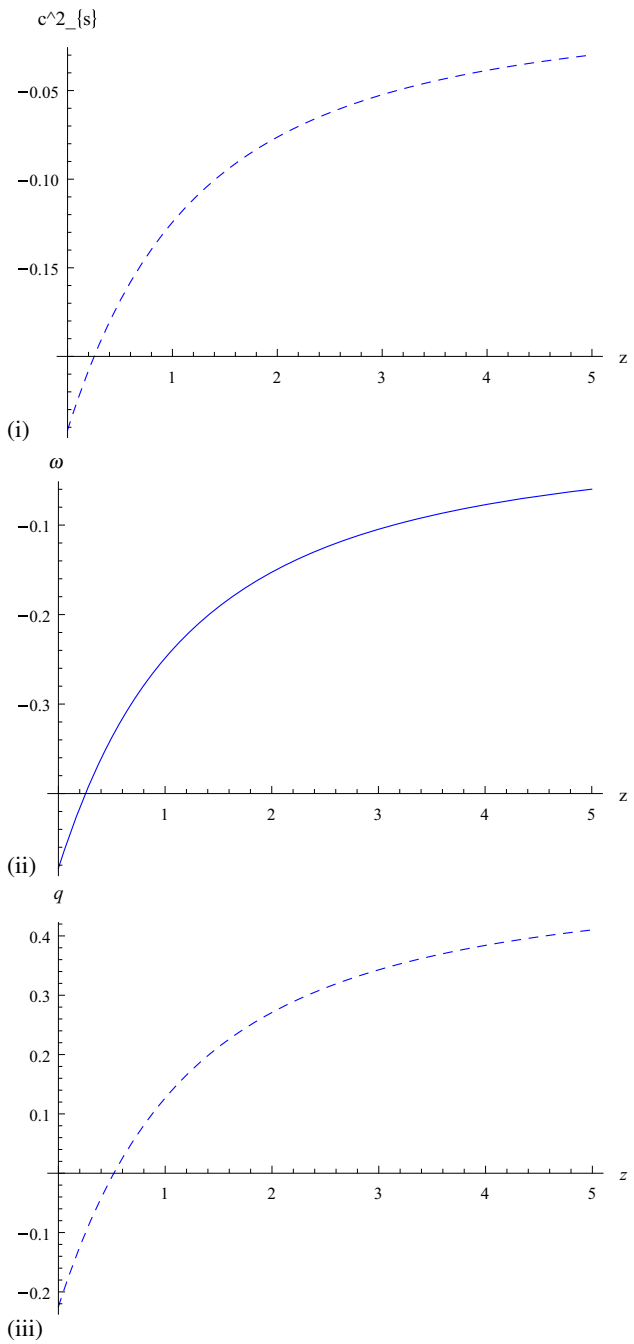

Figure 6. Plot of (**i**) the squared adiabatic sound speed c_s^2, (**ii**) EoS parameter ω and (**iii**) deceleration parameter q with redshift for the EU model with $A = 0$ in OU data.

are $H_0 = 67.90$, $A = -0.028$ and $\Omega_m = 0.256$ in the general EU model and $H_0 = 67.457$, $\Omega_m = 0.267$ in a particular EU model ($A = 0$). Here, in the general EU model, the present value of Hubble parameter is slightly higher and the present matter density is slightly lower than the model with $A = 0$. The present Hubble values predicted by our analysis are close to Planck 15 data [48].

(ii) The present observed data permit an EU scenario with $A \to 0$ and $A = 0$ which is evident from the plot of the state parameter (figures 5 and 6). The plot of deceleration parameter q (shown in figure 5) shows the presence of dark energy in this model with $A \to 0$.

(iii) In figures 5 and 6, the plot of the state parameter with z shows that $\omega \leq -\frac{1}{3}$ at the present

epoch which confirms an accelerating phase of the Universe.

(iv) Figures 5 and 6 show the variation of deceleration parameter with red-shift z. It is evident that in the recent past the Universe transits from deceleration phase to accelerating phase.

(v) In the general EU model, values of ω and q are more negative than in the $A = 0$ model indicating the possibility of higher acceleration in the former case.

(vi) In the general EU model, the present age of the Universe t_0 is 13.93 Gyr and in the EU model with $A = 0$, $t_0 = 13.50$ Gyr.

(vii) Plot of squared adiabatic sound speed c_s^2 in the general EU model (figure 5) and in the specific EU model ($A = 0$) (figure 6) shows a tendency towards positivity at higher red-shift thereby hinting at structure formation. This tendency is more in specific EU model ($A = 0$).

The analysis permits an EU model with $A \approx 0$, accommodating dust and dark energy as its constituents. The EU model with $A = 0$ is equally valid and in some aspects (t_0, c_s^2) it gives better results than general EU model. So, an EU model is viable in accordance with the background tests conducted.

The ΛCDM model works remarkably well at large scale but it has some problems in describing structures (cusp/core (CC) problem, missing satellite problem (MSP)) at small scales. The problems at small scales come from the vanishing pressure of dark matter (DM). EU model in standard gravity is one of the models that unify DM and dark energy and its EoS is different from ΛCDM. This EU starts from the static phase in the past and hence avoids the problems at small scales. In this study, it is found that the determined values of EoS parameters go with the observations. So, EU model is worthy of being treated as an alternative model of ΛCDM model.

Acknowledgements

The author would like to thank IUCAA Reference Centre at North Bengal University for extending necessary research facilities to initiate the work.

References

[1] A A Penzias and R W Wilson, *Astrophys. J. Lett.* **142**, 419 (1965)
[2] R H Dicke, P J E Peebles, P J Roll and D T Wilkinson, *Astrophys. J. Lett.* **142**, 414 (1965)
[3] A H Guth, *Phys. Rev. D* **23**, 347 (1981)
[4] K Sato, *Mon. Not. R. Aston. Soc.* **195**, 467 (1981)
[5] A Linde, *Phys. Lett. B* **108**, 389 (1982)
[6] A Albrecht and P Steinhardt, *Phys. Rev. Lett.* **48**, 1220 (1982)
[7] A G Riess *et al*, *Astron. J.* **116**, 1009 (1998)
[8] J L Tonry *et al*, *Astrophys. J.* **594**, 1 (2003)
[9] S Perlmutter *et al*, *Nature* **391**, 51 (1998)
[10] S Perlmutter *et al*, *Astrophys. J.* **517**, 565 (1999)
[11] A Albrecht, arXiv:astro-ph/0007247 (2000)
[12] S M Carroll, *Living Rev. Rel.* **4**, 1 (2001)
[13] S Mukherjee, B C Paul, N K Dadhich, S D Maharaj and A Beesham, *Class. Quantum Grav.* **23**, 6927 (2006)
[14] G F R Ellis and R Maartens, *Class. Quantum Grav.* **21**, 223 (2004)
[15] E R Harrison, *Mon. Not. R. Astron. Soc.* **69**, 137 (1967)
[16] Y F Cai, M Li and X Zhang, *Phys. Lett. B* **718**, 248 (2012)
[17] Y F Cai, Y Wan and X Zhang, *Phys. Lett. B* **731**, 217 (2014)
[18] B C Paul and S Ghose, *Gen. Relativ. Gravit.* **42**, 795 (2010)
[19] S Nojiri and S D Oddintsov, *Phys. Lett. B* **631**, 1 (2005)
[20] A Banerjee, T Bandyopadhyay and S Chakraborty, *Gen. Relativ. Gravit.* **40**, 1603 (2008)
[21] U Debnath, *Class. Quantum Grav.* **25**, 205019 (2008)
[22] S del Campo, R Herrera and P Labrana, *J. Cosmol. Astropart. Phys.* **30**, 0711 (2007)
[23] S Nojiri and S D Oddintsov, *Phys. Rev. D* **71**, 063004 (2005)
[24] A V Astashenok, S Nojiri, S D Oddintsov and A V Yurov, *Phys. Lett. B* **709**, 396 (2012)
[25] S Bag, V Sahni, Y Shtanov and S Unnikrishnan, arXiv:1403.4243 (2014)
[26] N Suzuki *et al*, *Astrophys. J.* **746**, 85 (2012)
[27] Z Li, W Puxun and Y Hongwei, *Astrophys. J.* **744**, 176 (2012)
[28] X Lixin, W Yuting and N Hyerim, *Eur. Phys. J. C* **72**, 1931 (2012)
[29] D J Eisenstein *et al*, *Astrophys. J.* **633**, 560 (2005)
[30] E Komatsu *et al*, *Astrophys. J. Suppl.* **192**, 18 (2011)
[31] C Zhang *et al*, *Res. Astron. Astrophys.* **14**, 1221 (2014)
[32] R Jimenez *et al*, *Astrophys. J.* **593**, 622 (2003)
[33] J Simon *et al*, *Phys. Rev. D* **71**, 123001 (2005)
[34] M Moresco *et al*, *J. Cosmol. Astropart. Phys.* **8**, 6 (2012)
[35] E Gaztanaga *et al*, *Mon. Not. R. Astron. Soc.* **399**, 1663 (2009)
[36] C-H Chuang *et al*, *Mon. Not. R. Astron. Soc.* **426**, 226 (2012)
[37] X Xu *et al*, *Mon. Not. R. Astron. Soc.* **431**, 2834 (2013)
[38] C Blake *et al*, *Mon. Not. R. Astron. Soc.* **425**, 405 (2012)
[39] D Stern *et al*, *J. Cosmol. Astropart. Phys.* **1002**, 008 (2010)
[40] L Samushia *et al*, *Phys. Rev. D* **86**, 103527 (2012)
[41] M Moresco, *Mon. Not. R. Astron. Soc.* **450**, L16 (2015)

[42] N G Busca *et al*, *Astron. Astrophys. A* **552**, 96 (2013)
[43] T Delubac *et al*, *Astron. Astrophys. A* **574**, 59 (2015).
[44] A Font-Ribera *et al*, *J. Cosmol. Astropart. Phys.* **5**, 27 (2014)
[45] G Hinshaw *et al*, *Astrophys. J. Suppl.* **208**, 19 (2013)
[46] C Blake *et al*, *Mon. Not. R. Astron. Soc.* **418(3)**, 1707 (2011)
[47] C-H Chuang *et al*, *Mon. Not. R. Astron. Soc.* **433(4)**, 3559 (2013)
[48] Planck Collaboration: P A R Ade *et al*, arXiv:1502.01589 [astro-ph.CO] (2015)